

Lessons Learned on Device Free Localization with Single and Multi Channel Mode

Pietro Cassarà*, Francesco Potorti*, Paolo Barsocchi*, Michele Girolami*[¶], Paolo Nepa[§]

*ISTI institute of CNR, via Moruzzi 1, 56124 Pisa, Italy

Email: {cassara,potorti,paolo.barsocchi,girolami}@isti.cnr.it

[§]Department of Information Engineering, University of Pisa, Via Caruso 16, 56122 Pisa, Italy

Email: paolo.nepa@iet.unipi.it

[¶]Department of Computer Science Largo B. Pontecorvo 3, 56127 Pisa, Italy

Abstract—Indoor localization applications that involve Wireless Sensor Networks (WSNs) identify the target position by measuring the Received Signal Strength (RSS), the Time of Arrival (ToA), the Time Difference of Arrival (TDoA) or the Angle of Arrival (AoA). Of these, the most promising for low-cost applications are those based on measures of the RSS, which exploit the relationship between RSS and the distance, or more reliably the relation between the multi-path interference (shadowing) and the position of the target. These methods work with WSNs based on Wi-Fi, Bluetooth and ZigBee sensor technologies.

In this paper we concentrate on *device-free* RSS-based indoor localization methods. These methods, which have generated much research interest in the last few years, are now starting to hit the market. Specifically, the purpose of this paper is to assess the performance improvements of a Variance-based Radio Tomographic Imaging technique, when scanning various radio channels with respect to using only one, the latter being the “minimum introduced interference” option.

Moreover, in this paper we will discuss in which application scenario the multi-channel scanning technique is usable and appropriate. The experimental data used for target localization are captured by wireless sensors deployed in the localization area and the localization error metrics include the mean square error and percentiles of the error distribution. Specifically, we aim to study the localization error reduction obtained by using multiple ZigBee channels, with respect to using a single channel.

I. INTRODUCTION

RELIABLE, accurate and real-time indoor positioning services and protocols are required in the future generation of communication networks [1]. A positioning system enables a mobile device available for positioning-based services such as tracking, navigation or monitoring. Moreover, information of the users position could significantly improve the performance of wireless networks for network planning [2], load balance [3], etc.

Localization and tracking of objects can be achieved by means of a large number of different technologies, however only few of them are suitable for Ambient Assisted Living (AAL) applications, since they should be non-invasive on the

users, they must be suited to the deployment in the user houses at a reasonable cost, and they should be accepted by the users themselves [4], [5].

Considering these constraints, a promising technology is based on Wireless Sensor Networks (WSN), due to their low cost and easy deployment. Within WSNs, it is possible to estimate the location of a user by exploiting the Received Signal Strength (RSS), the Time of Arrival (ToA), the Time Difference of Arrival (TDoA) or the Angle of Arrival (AoA).

Of these, the most promising for low-cost applications are those based on RSS measures, which is a measure of the power of a received radio signal that can be obtained from almost all wireless communications devices we know of.

The RSS measured among fixed devices (whose position is known) and mobile devices (carried by the user) is leveraged by algorithms that estimate the coordinates of the user positions. In a smart environment, where the ambience is instrumented with sensors and wireless communication devices, the marginal cost of implementing an RSS-based localization system can be very low, as it can leverage the existing installed hardware.

In this paper, we consider one device-free RSS-based indoor localization method, that is, Variance-based Radio Tomography Imaging (VRTI) [6]. Here, “device-free” means that a person does not need to carry or wear any wireless sensor or device. Rather, these systems are based on a large set of small wireless devices spread over the area of interest in order to create a dense mesh, and exploit the RSS observed by each device on the radio links connecting it to other devices. A user moving within the area modifies the RSS pattern in a way that depends on his location; radio imaging therefore exploits the RSS measurements observed along the inter-device links to obtain a reconstruction of the object trajectory. Two working modes can be identified for these devices: either they dedicate some power and channel occupancy to sending ad hoc localization probing packets, or else they exploit data packets sent by other applications and measure their RSS for localization purposes. Using a single radio channel for scanning is friendly to other devices in the environment, both in the case of dedicated localization devices and in the case of piggy-backing on different applications. In the former case,

This work was supported by the project Energia da fonti rinnovabili e ICT per la sostenibilità energetica; sottoprogetto Smart Building of the DIITET Department of CNR (Italy) and by the POR CRO FSE 2007-2013 research program. 978-1-4673-8402-5/15/\$31.00 2015 IEEE

having a dedicated channel avoids interference and channel occupancy for other applications in the same environment. In the latter, since no ad hoc packets are generated, there is no additional channel occupancy and energy drain.

On the other hand, results for a similar method, that is Shadowing-based RTI, showed that sending probing packets on multiple channels gives an advantage in terms of localization accuracy with respect to using a single channel [7]. This means that at least in some device-free systems there is a trade-off between minimum disturbance and maximum accuracy when choosing between single- and multiple-channel localization. Here we use the same criterion applied to VRTI [8], in order to measure if any performance improvements are observed with this method.

The remainder of the paper is articulated as follows: Section II presents the related work; Section III discusses the scenario and the experimental setup; Section IV describes the detail of the tomographic localization algorithm, while Section V presents some preliminary results; concluding remarks are given in Section VI.

II. RELATED WORK: DEVICE-FREE LOCALIZATION TECHNIQUES

Device-free radio localization methods based on RSS as provided by small and inexpensive communications sensors is a field that has gained growing interest in the last few years. Indeed, previous works show that changes in link path losses can be used to accurately estimate an image of the attenuation field, that is, a spatial plot of attenuation per unit area [9]. Experimental tests show that in an unobstructed area surrounded by a network of nodes, the estimated image displayed the positions of people in the area. Indoor radio channel characterization research demonstrates that objects moving near wireless communication links cause variance in RSS measurements [10]. This knowledge has been applied to detect and characterize motion of network nodes and moving objects in the network environment [11]. These studies focus mostly on detection and velocity characterization of movement, but do not attempt to localize the movement as the works presented in this section.

Device-free localization systems are characterized by the absence of any kind of devices wear by the user which actively emit any useful signal. These localization systems are particularly useful in medical, data-mining or ambient assisted living applications where a huge number of person need to be localized and tracked, or in security, military applications, where the users don't want to be localized.

These systems are based on large set of small wireless devices spread over the area of interest in order to create a dense mesh, and exploit the RSS observed by each device on the links connecting it to other devices. A user moving within the area modifies the RSS pattern in a way that depends on his location; the algorithms exploit the RSS measurements observed along the inter-device links to obtain a reconstruction

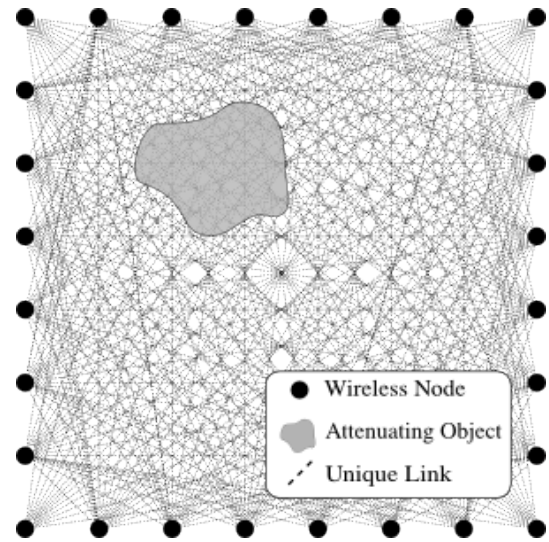


Fig. 1. Principle of device-free localization systems.

of the object trajectory (figure 1¹). As far as we know four different device-free localization techniques are already published in the literature: Radio Imaging (RI) [12], Massa's method [13], REAAL method [14], and Variance-based Radio Tomography Imaging (VRTI) [6].

In [12] the authors propose an approach where both the average path-loss and the fluctuations of the received signal strength induced by the moving target are jointly modeled based on the theory of diffraction. The device-free localization problem is cast into a Bayesian framework based on a stochastic model that allows to describe the target-induced RSS perturbations and optimally exploits all the location information coming from attenuation, random fading and mobility model. A stochastic model is proposed for relating the RSS measurements over each link to the object position. Since the presence of the target is shown to affect both the attenuation and the random fluctuations of the received power, a log-normal model is defined where the RSS mean and variance are expressed as functions of the target location. The increase of path-loss and power fluctuation induced by the moving target are described by exploiting the theory of diffraction: a closed-form analytical model is derived, tailored for the specific localization problem and validated on experimental data.

In [13] the measurement of the perturbation effects on the other receiving nodes is dealt with a suitable inversion strategy to determine the equivalent source modeling the presence of the target/scatterer generating the perturbation itself. By virtue of the fact that the number of nodes in a WSN can vary and the need to have a simple and flexible tracking/localization method allowing real-time estimates, a learning-by-examples (LBE) strategy based on a support vector machine (SVM) is used.

¹Taken with permission of Neal Patwari from <http://span.ece.utah.edu/radio-tomographic-imaging?q=radio-tomographic-imaging>

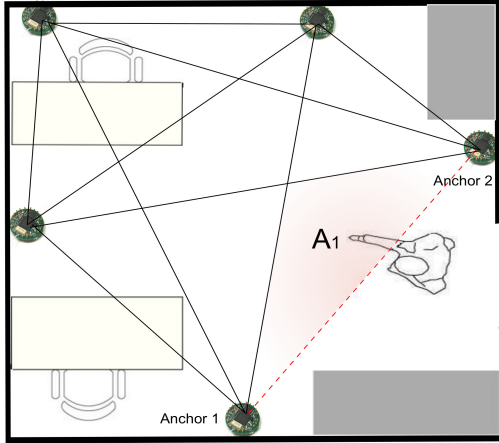


Fig. 2. REAAL algorithm: AAL compliant device-free localization system.

The authors in [14] propose a method based on identify the signal fading between two anchors. Indeed, a user crossing the Line-of-Sight (LOS) link between two anchors causes signal fading through the link. Identifying power reduction on a given radio link can be exploited to know the area where the user is going into. As shown in figure 2, if the user enters the room and the detection algorithm detects that the LOS link between anchors 1 and 2 is affected, the localization system infers that the user is entering the subarea A_1 , and will indicate the coordinates of the centroid of that subarea. This method is particularly indicated for AAL environment where good user acceptance is essential since it is able to estimate in advance the maximum error and it works even with a small number of installed devices.

The method proposed in [6] takes advantage of the motion-induced variance of received signal strength measurements made in a wireless peer-to-peer network. Indeed, using a multipath channel model, the authors show that the signal strength on a wireless link is largely dependent on the power contained in multipath components that travel through space containing moving objects. Exploiting measurements from many links in the wireless network, the authors present a statistical model relating variance to spatial locations of movement and used as a framework for the estimation of a motion image. From the motion image, the Kalman filter is applied to recursively track the coordinates of a moving target. The achieved mean accuracy is usually around half meter, which is enough for AAL applications, where 50 cm can be considered acceptable [4], [15]. We chose this method to asses the performance improvements when scanning several radio channel since it is the most promising device-free localization algorithm. A clear and more exhaustive description of this algorithm is given in section IV.

The two main drawbacks of these device-free methods are the large number of devices that must be deployed in the environment and the incapability of discriminating among

users. Association with a sufficiently smart tracking system may help with the first problem, while a complete solution is only possible in association with other techniques (usually non device-free, like RFID).

III. EVALUATION SCENARIO

In this section we introduce the software, the hardware devices and the scenario used during our analysis. The RSS values are collected through a WSN composed by N nodes in the following named as *anchors*.

A. Software Tool

A modified version of token-passing protocol, named as Spin [16], is used to schedule node transmission, in order to prevent packet collisions and maintain high data collection rate. When an anchor is transmitting, all other anchors receive the packet and perform the RSS measurements. The payload of the transmitting packet is the set of RSS values between the transmitting node and the other sensors sampled during the previous cycle. This packet has been received also by the base station along with the nodes unique ID. The base station collects the payload and forwards this data to a laptop for storage and later processing. The RSS values are acquired for a given channel c for all the nodes $n = 1 \dots N$ in the network, i.e., when the last node of the network has transmitted by using the channel c , the first sensor node starts with a new cycle by using a new channel. The data collected from each sensor pair

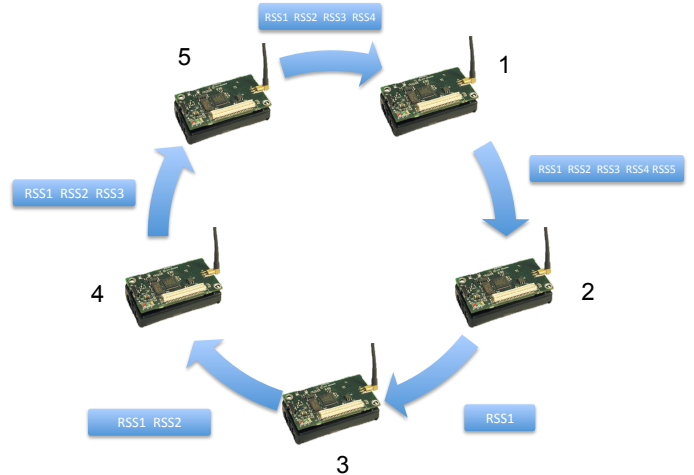


Fig. 3. Software toll used in the measurement campaign.

(a_i, a_j) in the following called *link*, are formatted as a string with the following fields: the identifier of the receiver (ID), the RSS values measured between the receiver and the others transmitting sensors, the timestamp at which the string was acquired, and finally the channel used for the acquisition. It is worth noting that in the literature taken into account for this paper the authors drop the assumption on the reciprocity of the links.

B. Hardware

The WSN used in this work is based on the IRIS Motes wireless sensor nodes, produced by Crossbow [17]. This hardware is based on the high performance RF transceiver, AT86RF230, operating at 2.4GHz compliant with the IEEE 802.15.4 and ZigBee standards. The hardware was programmed using the TinyOS operating system, specifically designed for low-power wireless devices. The AT86RF230 can return the instantaneous RSS and the average RSS values through two registers named *RSS_Val* and *ED register*, respectively. The first one is a 5-bits bit register, the second one is a 8-bit register.

C. Experimental Setup

The RSS values were collected in the presence of a human target (from now on named simply target) in a set of given positions. The localization area is about 4.8 x 3.6 meters where 20 sensors have been placed for the data acquisition. The measures are performed on a set of 1, 2 and 4 channels.

Each link is sampled with a frequency between 5 and 8 Hz, depending on the parameters used in the algorithm described in section IV. The target movement was a sort of serpentine as shown in Figure 4 at a constant speed of about 0.2 m/s. The RSS data collected during each experiment consist of more than 5600 cycles, corresponding to more than 112000 RSS measures among anchors. Furthermore, no one other than the user to be localized is present in the area during the experiment.

The localization area of each scenario was marked to create a lattice, as shown in the figure 4, where the black squares are the WSN nodes. Through this lattice the position of the target has been evaluated, and comparing estimated position with the target's position in the lattice the localization error distribution is evaluated. From the error distribution the root mean square error (RMSE), the 75th and 90th percentile of the localization error are calculated.

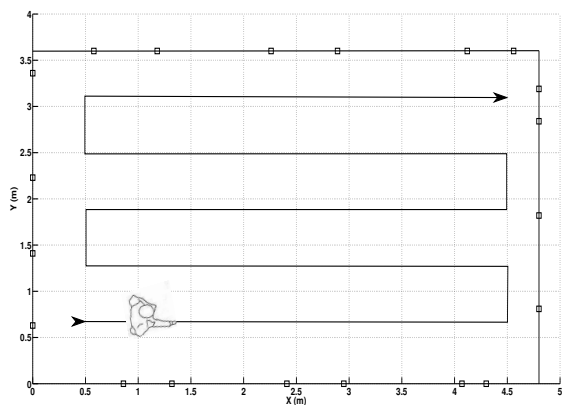


Fig. 4. Environment setup: N=20 anchors positioned near the room walls, at about 70 cm from the floor, and the path followed by the target.

IV. ALGORITHM

The algorithm is an implementation of the Variance-based Radio Tomographic Imaging (VRTI) method [9]. In the RTI algorithm the data used for the imaging are the RSS levels collected for each pair of wireless devices of the wireless sensor network deployed within the localization area.

The VRTI algorithm uses the path loss of the radio links between many pairs of nodes in a wireless network, in order to image the attenuation changes that occur within the localization area. In general, when an object moves into the localization area, the signal strength of the link involved in the target path will, on average, experience higher shadowing losses. VRTI is an inverse problem based on the path loss on the intersecting links, by which the image of the attenuation within the localization area is reconstructed to infer the location of the target. In the following we shortly describe how it works.

Consider the set of anchors $A = a_1, a_2, \dots, a_n$ with known positions on the localization area; all the anchor pairs identify the L links of the wireless sensor network. In the localization area, a lattice with P pixels is introduced, and for each pixel its coordinates within the lattice are evaluated.

The first step for the evaluation of the attenuation image over the localization area consists in evaluating the matrix of the variance weighting, which links the RSS's variance of the link to the variance over the pixels, as shown in equation (1).

$$\mathbf{s} = \mathbf{W}\mathbf{x} + \mathbf{v} \quad (1)$$

In equation (1) \mathbf{x} is the image vector that holds the values per pixel of the RSS's variance, \mathbf{s} is the vector that holds the measured RSS's variance per link, \mathbf{v} is the noise vector, and \mathbf{W} is the matrix representing the variance weighting for each pixel and link.

The entries of the matrix \mathbf{W} are calculated by assuming that the signal strength between nodes pair decays with the inverse square of the distance between two nodes, and that the movement of the target influences the set of pixels included in the ellipse shown in figure 5, whose foci are the nodes a_i and a_j , while λ , defined as $d_{lp}(1) + d_{lp}(2) - d_l$, controls the ellipse eccentricity. Equation (2) shows how to evaluate the entries of the matrix \mathbf{W} .

$$W_{lp} = \frac{1}{\sqrt{d_l}} \begin{cases} \Psi & d_{lp}(1) + d_{lp}(2) \leq d_l + \lambda \\ 0 & \text{otherwise} \end{cases} \quad (2)$$

In equation (2) d_l is the distance of the link l between node pair (a_i, a_j) , $d_{lp}(1)$ and $d_{lp}(2)$ are the distances from the center of pixel p to the two respective nodes location on link l , and Ψ is a normalization parameter. For the scenarios analyzed in this paper some measurements have been performed to tune the parameters Ψ and λ , and the optimized values are 1 [dB]² and 1 m, respectively.

The output of the implemented VRTI algorithm is the vector image \mathbf{x} of equation (1). The vector \mathbf{x} can not be calculated through the equation (1) because it is an ill-posed inverse

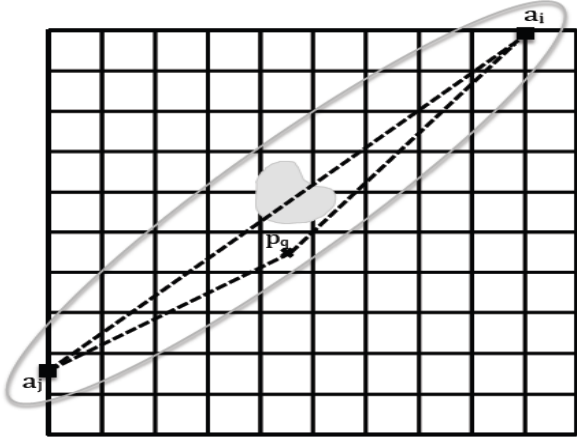


Fig. 5. Attenuation Area.

problem, hence, no unique solution to the least-squares formulation exists. The solution can be determined only through the resolution of a regularization problem; here, Tikhonov's least squares regularization problem was used [18], which can be formulated as in equation (3).

$$\hat{\mathbf{x}} = \arg \min_{\mathbf{x}} \frac{1}{2} \|\mathbf{W}\mathbf{x} - \mathbf{s}\|^2 + \alpha \|\mathbf{Q}\mathbf{x}\|^2 \quad (3)$$

The equation of the regularization problem involves the matrix \mathbf{Q} and the parameter α that are the Tikhonov matrix and the Tikhonov parameter, respectively. In many cases, this matrix \mathbf{Q} is chosen as the identity matrix $\mathbf{Q} = \mathbf{I}$, giving preference to solutions with smaller norms. In other cases, low-pass operators (e.g., a difference operator or a weighted Fourier operator) may be used to enforce smoothness if the underlying vector is believed to be mostly continuous. This regularization improves the conditioning of the problem, thus enabling a numerical solution. The parameter α affects the convergence of the algorithm and can be evaluated by the numerical method described in [18].

In our case, the measured data \mathbf{s} are subject to errors and these errors can be assumed to be independent with zero mean and standard deviation σ_v . Moreover, the a priori uncertainties of the solution \mathbf{x} can be taken into account through the covariance matrix \mathbf{C} . Then the solution for the regularization problem can be formulated as shown in equation (4), in terms of the a priori information \mathbf{C} and the noise variance σ_v^2 [18] [6].

$$\hat{\mathbf{x}} = (\mathbf{W}^T \mathbf{W} + \sigma_v^2 \mathbf{C}^{-1})^{-1} \mathbf{W}^T \mathbf{s} \quad (4)$$

$$C_{p_r p_q} = \sigma^2 e^{-d_{p_r p_q} / \delta}$$

Precisely, the correlation between the attenuation over the pixel set can be calculated using an exponential spatial decay law. In this case, the variable $d_{p_r p_q}$ is the distance from center of pixel p_r to the center of pixel p_q , σ^2 is the variance of pixel attenuation, and δ is used to determine the desired amount of smoothness in the image. Hence equation (4) achieves the

image reconstruction. For the scenarios analyzed in this paper the values of the parameters σ^2 and δ have been set to 0.3 and 3, respectively.

Then, the second step of the algorithm is to evaluate the solution of the regularization problem as described above.

The vector $\hat{\mathbf{x}}$ is used to estimate the target coordinates, selecting its maximum, and calculating the coordinate of the pixel with the maximum degree of attenuation. So, the final step of the algorithm is to show the image reconstruction $\hat{\mathbf{x}}$ through a color map, and the estimated coordinate of the target position compared with the true position, depicted by a circle and a cross respectively, as shown in figure 6. The color degrees of the figure indicate the different levels of attenuation due to the target movement over the lattice pixels.

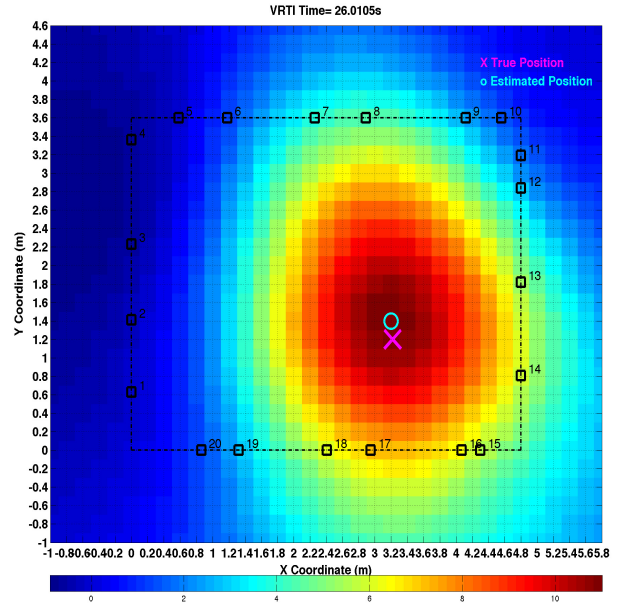


Fig. 6. VRTI Example.

V. RESULTS

We used several criteria to try and compare the performance of single- versus multi-channel, as detailed in the following four sub-sections.

A. Simple and bare comparison

Here we simply compare the performance of measurements done in single-channel mode on four different channels, with measurements done in bi-channel and quadri-channel mode, for a total of six cases.

The packet generation rate is around 55 pkt/s, which means one complete round of the 20 transmitting nodes in about 345 ms, or about three complete rounds per second. The window over which the RSS variance is measured is set at 3 s and 5 s, which means that the same measured data are used twice, and two sets of results are obtained. Note that the speed of the target is around 0.2 m/s meaning that, space-wise, the variance window is respectively 0.6 m and 1 m long for

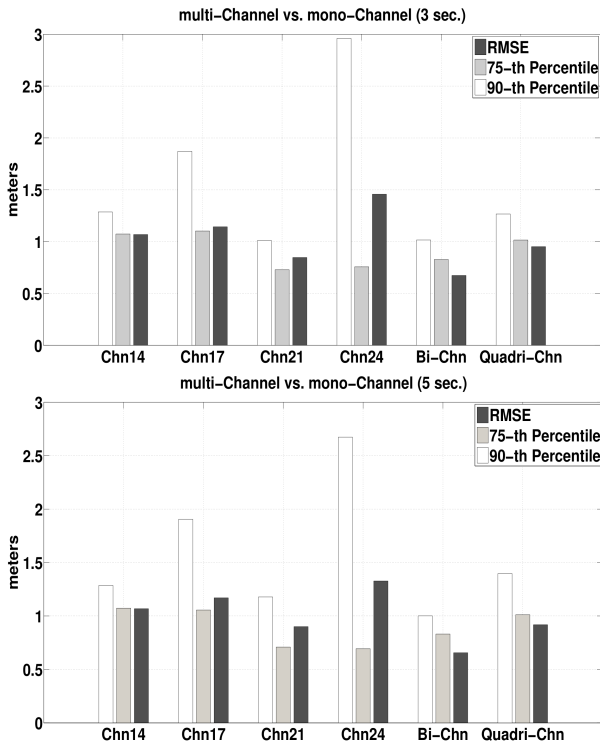


Fig. 7. Main comparison: single-channel performance for channels 14, 17, 21, 24 compared with bi-channel (17, 25) and quadri-channel (12, 16, 20, 24). 3 s and 5 s variance windows.

the two cases. In general, we expect to get a localization error not significantly smaller than the window size.

As shown in figures 7, we have found little difference between single-channel, bi-channel and quadri-channel measurements. The performance metrics we used are the RMSE (root mean square error) and two percentiles (75 and 90) of the localization error distribution. As an example, figures 8 show some typical error distribution for our experiments.

Note that the comparison in figure 7 is not rigorous, because it is based on six different measurements. This means that interference from radio sources may be different in the six measurements. Additionally, the actor's movement may be slightly different in the six measurements and people moving in nearby rooms may also have differently influenced the measurements. These issues are tackled in the next subsection.

B. Filtering comparison

In order to remove the effect of possible differences between different measurements when comparing single- to multi-channel performance, we make a comparison that uses a single bi-channel measurement (the same as the one depicted in figure 7) and filter it in three different ways like shown in figure 9.

The purpose is to extract from a single measurement set a bi-channel trace and two single-channel traces, all of them with the same number of samples per second, so that a comparison among them is significant.

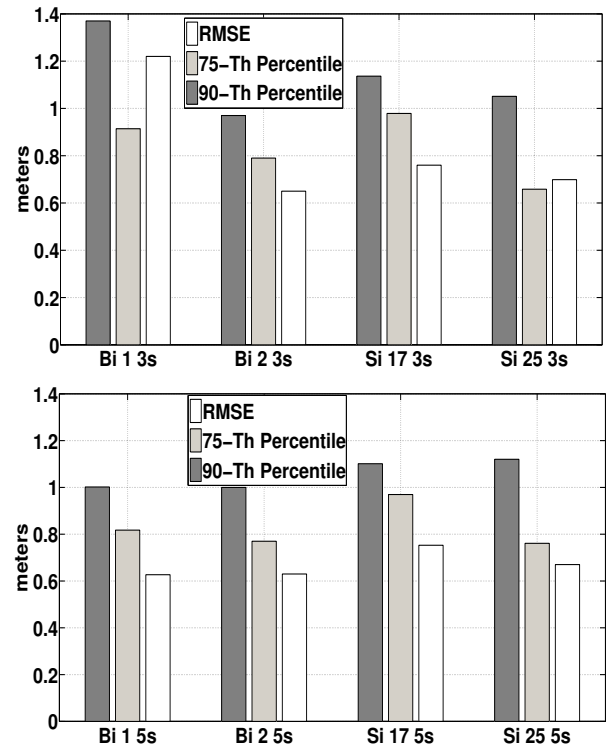


Fig. 11. Rigorous comparison: filtering bi-channel and single-channel from a bi-channel measurement. 3 s and 5 s variance windows.

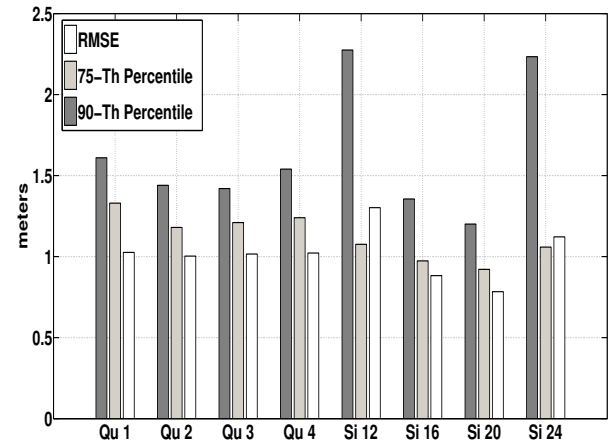


Fig. 12. Rigorous comparison: filtering quadri-channel and single-channel from a quadri-channel measurement. 10 s variance window.

We used the same procedure starting from a quadri-channel measurements that we filtered in five different ways (see figure 10).

We should consider this filtering procedure as the most rigorous of the tests we made. Its main drawback is that the number of samples per second is reduced by two times in the bi-channel case and by four times in the quadri-channel case, which stretches the RTI algorithm ability to its limits. Figures 11 and 12 show the resulting comparison.

Again, we do not perceive any significant difference when

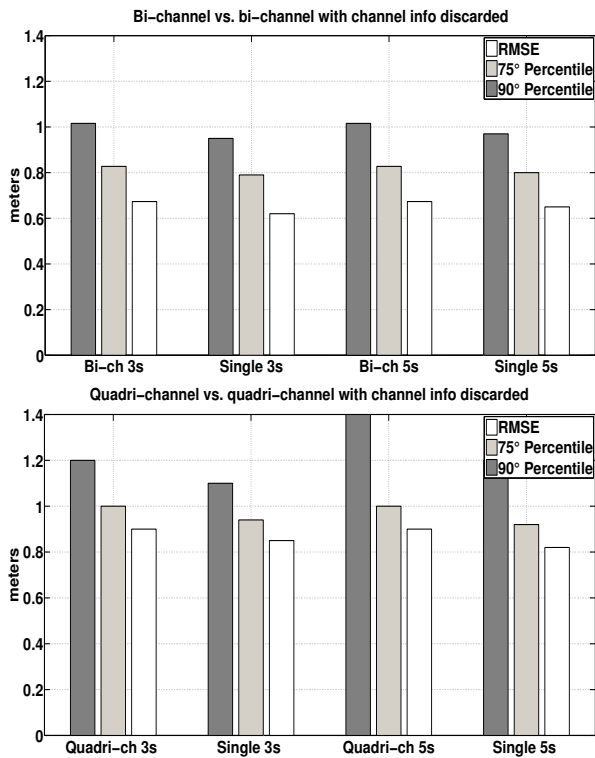


Fig. 13. Discarding channel information: treating multi-channel data as if they were single-channel do not significantly worsen the performance.

comparing single- and multi-channel performance.

C. Removing multi-channel information

As one more criterion to check for the importance of measurements over different channels, we took a quadri-channel measurement and removed the channel information. In practice, we made the measurements on four different channels and run the algorithm on the complete data, including channel information, as well as on the data where the channel information has been removed (so all the samples appear to have been logged on the same channel). Before making the comparison, we cared about removing the mean value individually from each channel's data, in order to avoid spurious variance introduced by mixing different channel's data. The results are depicted in figure 13 and, again, do not indicate any significantly worse performance when the channel information is discarded.

D. Treating single-channel as multi-channel

As a last test, we "invented" multi-channel information and added it to single-channel measurements. This test is a sort of security check that we did to verify that our implementation of the VRTI algorithm did not introduce any artifacts that advantage the single- or the multi-channel measurements. In figure 14 we observe a small improvement when "inventing" channel information.

VI. CONCLUSION

Measurement results relevant to an RTI-based localization technique have been presented and discussed. Main goal was showing whether using multiple radio channels for collecting RSSI samples is advantageous with respect to using only one frequency channel, as far as variance-based RTI localization is concerned. We used several criteria to compare the performance of single- versus multi-channel approach in order to evaluate all the possible solutions and reference scenarios. We conclude that using multiple channels may be more complex, especially if the packets are not explicitly generated for the purpose of localization, but just for communication purposes. In the latter case, the channel is constrained by communication protocols because of interference criteria or more generally by spectrum sharing criteria. Measurement results show that in this scenario is not convenient the multi-channel approach when using variance-based RTI localization algorithm, since there is not a significant improvement to justify the more complex system. Indeed, the main advantage of RSS-based localization systems is that they are totally free in smart environments, where the ambient is already instrumented with sensors and wireless communication devices that can be leveraged by the localization systems. Any change in the communication protocol, such as multi-channel scanning, are expensive and it brings small benefit. On the other hand, if an environment need to be sensorized with new devices with the localization purposes, then we can dedicate some power and channel occupancy to sending ad hoc localization probing packets in multi-channel way in order to improve the localization accuracy with respect to single-channel approach.

REFERENCES

- [1] C. Di Flora, M. Ficco, S. Russo, and V. Vecchio, "Indoor and outdoor location based services for portable wireless devices," in *Distributed Computing Systems Workshops, 2005. 25th IEEE International Conference on*, 2005, pp. 244–250.
- [2] B. Rao and L. Minakakis, "Evolution of mobile location-based services," *Commun. ACM*, vol. 46, no. 12, pp. 61–65, Dec. 2003. [Online]. Available: <http://doi.acm.org/10.1145/953460.953490>
- [3] E. Yanmaz and O. Tonguz, "Location dependent dynamic load balancing," in *Global Telecommunications Conference, 2005. GLOBECOM '05. IEEE*, vol. 1, 2005, pp. 5 pp.–.
- [4] J. A. Álvarez-García, P. Barsocchi, S. Chessa, and D. Salvi, "Evaluation of localization and activity recognition systems for ambient assisted living: The experience of the 2012 evala competition," *Journal of Ambient Intelligence and Smart Environments*, vol. 5, no. 1, pp. 119–132, 01 2013. [Online]. Available: <http://dx.doi.org/10.3233/AIS-120192>
- [5] P. Barsocchi, S. Lenzi, S. Chessa, and F. Furfari, "Automatic virtual calibration of range-based indoor localization systems," *Wireless Communications and Mobile Computing*, pp. n/a–n/a, 2011.
- [6] J. Wilson and N. Patwari, "Through-Wall Motion Tracking Using Variance-Based Radio Tomography Networks," *IEEE Transactions on Mobile Computing*, vol. 10, no. 5, pp. 612–621, May 2011.
- [7] N. Patwari, M. Bocca, and O. Kaltiokallio, "Enhancing the accuracy of radio tomographic imaging using channel diversity," *2012 IEEE 9th International Conference on Mobile Ad-Hoc and Sensor Systems (MASS 2012)*, vol. 0, pp. 254–262, 2012.
- [8] J. Wilson and N. Patwari, "Radio tomographic imaging with wireless networks," *Mobile Computing, IEEE Transactions on*, vol. 9, no. 5, pp. 621–632, 2010.
- [9] J. Wilson and N. Patwari, "Radio Tomographic Imaging with Wireless Networks," *IEEE Transactions on Mobile Computing*, vol. 9, no. 5, pp. 621–632, May 2009.

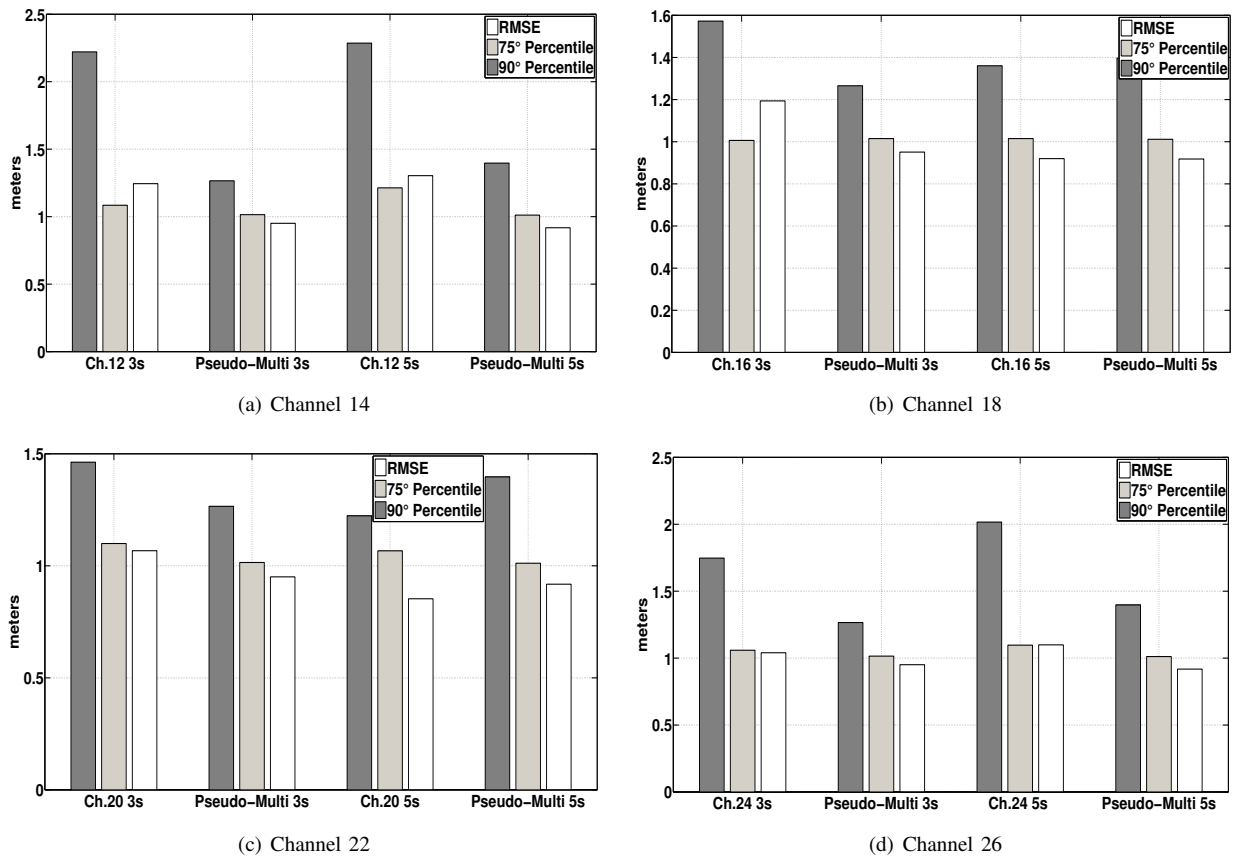


Fig. 14. Adding “invented” channel information: single-channel measurements are enriched with nonexistent multi-channel info.

- [10] R.J. Bultitude, “Measurement, Characterization, and Modeling of Indoor 800/900 MHz Radio Channels for Digital Communications,” *IEEE Comm. Magazine*, vol. 25, no. 6, pp. 5–12, June 1987.
- [11] K. Woyach, D. Puccinelli, and M. Haenggi, “Sensorless sensing in wireless networks: Implementation and measurements,” in *Second International Workshop Wireless Network Measurement (WinMee 06)*, 2006.
- [12] S. Savazzi, M. Nicoli, F. Carminati, and M. Riva, “A bayesian approach to device-free localization: Modeling and experimental assessment,” *Selected Topics in Signal Processing, IEEE Journal of*, vol. 8, no. 1, pp. 16–29, Feb 2014.
- [13] F. Viani, M. Martinelli, L. Ioriatti, L. Lizzi, G. Oliveri, P. Rocca, and A. Massa, “Real-time indoor localization and tracking of passive targets by means of wireless sensor networks,” in *Antennas and Propagation Society International Symposium, 2009. APSURSI '09. IEEE*, June 2009, pp. 1–4.
- [14] P. Barsocchi, F. Potorti, and P. Nepa, “Device-free indoor localization for aal applications,” in *Wireless Mobile Communication and Healthcare*, ser. Lecture Notes of the Institute for Computer Sciences, Social Informatics and Telecommunications Engineering, B. Godara and K. Nikita, Eds. Springer Berlin Heidelberg, 2013, vol. 61, pp. 361–368. [Online]. Available: http://dx.doi.org/10.1007/978-3-642-37893-5_40
- [15] P. Barsocchi, S. Chessa, F. Furfari, and F. Potorti, “Evaluating AAL solutions through competitive benchmarking: the localization competition,” *IEEE Pervasive Computing Magazine*, vol. 12, no. 4, pp. 72–79, Oct.–Dec. 2013.
- [16] J. Wilson and N. Patwari, “Spin: A token ring protocol for RSS collection,” <http://span.ece.utah.edu/spin>.
- [17] C. Technology, “IRIS Datasheet,” <http://bullseye.xbow.com:81>, 2013.
- [18] A. N. Tikhonov and A. V. Y., *Solution of Ill-posed Problems*. Washington: Winston & Sons, 1977.